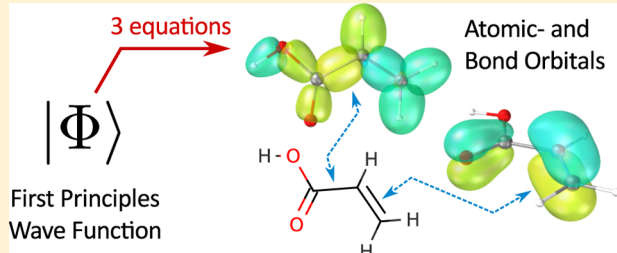


Intrinsic Atomic Orbitals: An Unbiased Bridge between Quantum Theory and Chemical Concepts

Gerald Knizia*

Institut für Theoretische Chemie, Universität Stuttgart, Pfaffenwaldring 55, D-70569 Stuttgart, Germany

ABSTRACT: Modern quantum chemistry can make quantitative predictions on an immense array of chemical systems. However, the interpretation of those predictions is often complicated by the complex wave function expansions used. Here we show that an exceptionally simple algebraic construction allows for defining atomic core and valence orbitals, polarized by the molecular environment, which can exactly represent self-consistent field wave functions. This construction provides an unbiased and direct connection between quantum chemistry and empirical chemical concepts, and can be used, for example, to calculate the nature of bonding in molecules, in chemical terms, from first principles. In particular, we find consistency with electronegativities (χ), C 1s core-level shifts, resonance substituent parameters (σ_R), Lewis structures, and oxidation states of transition-metal complexes.



1. INTRODUCTION

Chemical concepts as fundamental as atomic orbitals (AOs) in molecules, covalent bonds, or even partial charges do not correspond to physical observables; such concepts therefore cannot be unambiguously defined in pure quantum theory. This leads to some curious situations: for example, quantum chemistry methods can determine benzene's heat of formation with an accuracy of <2 kJ/mol,¹ but, strictly speaking, they can neither determine the partial charges on benzene's carbon atoms, nor can they show that benzene has twelve localized σ -bonds and a delocalized π -system. Chemical bonds have even been compared to unicorns: mythical creatures of which everyone knows how they look, despite nobody ever having seen one.²

However, qualitative concepts are of essential importance for practical chemistry, and thus a large number of competing techniques were developed for extracting them from quantum chemical calculations. In particular, Bader's atoms in molecules³ and Weinhold's natural atomic/bond orbital analysis (NAO/NBO)^{4,5} are widely used for interpreting molecular electronic structure. Nonetheless, the former is known to produce counterintuitive results in many cases,⁶ and the latter, while undoubtedly having brought countless successes in chemical interpretation, is complicated and preimposes various nontrivial assumptions. Concretely, NBO analysis is based on the two notions that (i) AOs in molecules have a spherical symmetry and can be obtained by a particular complex series of transformations,⁴ and (ii) a Lewis-like bonding pattern for any given molecule exists and only needs to be found—by comparing the wave function to all possible Lewis patterns.⁷ While normally applicable, violations of both assumptions are conceivable in unusual bonding situations, and might then lead to erratic interpretations. Energy decomposition and related techniques^{8–15} are also important and widely used in interpretation, but have different aims.

Here, we present a new technique to connect quantitative self-consistent field (SCF) wave functions to a qualitative

chemical picture. This technique is essentially free of empirical input, allows for computing the nature and shape of chemical bonds, and is not biased toward any preconceived notion of bonding. This is achieved by first defining a new intrinsic minimal basis (IMB),¹⁶ a set of perturbed core and valence AOs which can exactly describe the occupied molecular orbitals (MOs) of a previously computed SCF wave function. We will show that the intrinsic atomic orbitals (IAOs) thus defined can be directly interpreted as the *chemical* AOs, and that partial charges and bond orbitals (IBOs) derived from them perfectly agree with both experimental data and intuitive chemical concepts. In particular, we find a natural emergence of the Lewis structure of molecules.

Suggestions to use either unpolarized^{17–20} or polarized^{21–24} free-atom AOs to interpret molecular wave functions appeared early in the literature, and methods continue to be developed. Also, IMBs spanning occupied orbitals, as this work is concerned with, have been constructed before;^{16,25–31} a particularly advanced one was recently introduced by Laikov,³¹ who also discusses the literature in the field. However, despite the conceptual advantages of such IMB, so far none of them have found widespread use comparable to Bader or NAO analysis, and most are technically rather complex and have not been intensively tested with regard to empirical laws and facts. Our contribution is a IMB which is simple and efficient, its use in constructing bond orbitals, and the demonstration that this combination shows excellent promise for interpreting chemical bonding and reactivity. The technique thereby provides a firm quantum mechanical basis for ubiquitous fundamental concepts.

Received: August 1, 2013

Published: August 29, 2013



2. CONSTRUCTION OF INTRINSIC ORBITALS

Assume that we have computed a molecular SCF wave function $|\Phi\rangle$. $|\Phi\rangle$ is defined by its occupied MOs,

$$|i\rangle = \sum_{\mu} |\mu\rangle C_i^{\mu}$$

where $\mu \in B_1$ are basis functions from a large basis set B_1 . The key problem in interpreting wave functions is that the basis functions $|\mu\rangle$ cannot be clearly associated with any atom; each function will contribute most where it is most needed, and, because of B_1 's high variational freedom, this often is not on the atom it is placed on. On the other hand, if one were to expand the MOs over a minimal basis B_2 of free-atom AOs (i.e., a basis consisting of AOs calculated with sufficient radial freedom, but e.g., with only AOs 1s, 2s, 2px-2pz for each C atom), the wave function would be easy to interpret. But it would be inaccurate, and it might be even qualitatively incorrect, because free-atom AOs contain no polarization due to the molecular environment. We thus propose to first calculate an accurate wave function $|\Phi\rangle$, and then to form a set of polarized AOs $|\rho\rangle \notin B_2$ that can exactly express $|\Phi\rangle$'s occupied MOs $|i\rangle$.

For this, we first split the free-atom AOs $|\tilde{\rho}\rangle \in B_2$ into contributions corresponding to a depolarized occupied space $\tilde{O} = \sum_i |i\rangle\langle i|$ and its complement $1 - \tilde{O}$. Let

$$P_{12} = \sum_{\mu\nu \in B_1} |\mu\rangle S^{\mu\nu} \langle \nu| \quad P_{21} = \sum_{\rho\sigma \in B_2} |\rho\rangle S^{\rho\sigma} \langle \sigma|$$

denote the projectors onto the bases B_1 and B_2 , respectively, where $S^{\mu\nu}/S^{\rho\sigma}$ are inverse overlap matrices in B_1/B_2 . [Note that concerning projections from the minimal basis B_2 to the large basis B_1 , P_{12} is effectively an identity operator.] Then the depolarized MOs

$$\{|\tilde{i}\rangle\} = \text{orth}\{P_{12}P_{21}|i\rangle\} \quad (1)$$

are obtained by projecting the accurate MOs $|i\rangle$ from the main basis B_1 onto the minimal basis B_2 (which cannot express polarization) and back. As a consequence, $|\tilde{i}\rangle$ lies completely within the space spanned by $\{P_{12}|\tilde{\rho}\rangle, |\tilde{\rho}\rangle \in B_2\}$ and, thus, the free-atom AOs $P_{12}|\tilde{\rho}\rangle$ can be exactly split into one subspace corresponding to the occupied orbitals ($\text{span}\{\tilde{O}P_{12}|\tilde{\rho}\rangle\}$) and a second subspace corresponding to the virtual valence orbitals ($\text{span}\{(1 - \tilde{O})P_{12}|\tilde{\rho}\rangle\}$). We can then get the polarized AOs $|\rho\rangle$ from the free-atom AOs $|\tilde{\rho}\rangle$ by simply projecting their contributions in \tilde{O} and $1 - \tilde{O}$ onto their polarized counterparts $O = \sum_i |i\rangle\langle i|$ and $1 - O$:

$$|\rho\rangle = (O\tilde{O} + (1 - O)(1 - \tilde{O}))P_{12}|\tilde{\rho}\rangle \quad (2)$$

Thus, to construct the polarized AOs, it is sufficient to load a tabulated free-atom basis, calculate its overlap with the main basis and within itself, and perform the numerically trivial projection given by eq 2. Contrary to the related approach of ref 16, no functional optimization or reference to virtual orbitals is required. In this article, we will also symmetrically orthogonalize the vectors obtained via eq 2, to arrive at an orthonormal minimal basis that divides the one-particle space into atomic contributions; the latter will be referred to as intrinsic atomic orbitals (IAOs).

While the construction makes reference to free-atom AOs through basis B_2 , it must be stressed that these are *not* empirical quantities. Free-atom orbitals can be *calculated* with any high-level quantum chemistry program. However, in practice this is not even required, because they are already tabulated as part

of several standard basis sets; here, we take the AO functions of cc-pVTZ, which are spherically averaged ground-state Hartree–Fock orbitals. (Further technical comments on the IAO construction and the choice and nature of the free-atom orbitals are provided in Appendices B and C.)

Since IAOs are directly associated with atoms, they can be used to define atomic properties such as partial charges. Let us denote the closed-shell SCF density matrix as $\gamma = 2\sum_i |i\rangle\langle i|$, where i are the occupied MOs. We can then define

$$q_A = Z_A - \sum_{\rho \in A} \langle \rho | \gamma | \rho \rangle \quad (3)$$

as the partial charge on atom A, where Z_A is the atom's nuclear charge and ρ represents its IAOs. Table 1 shows that the partial

Table 1. Basis Set Convergence of Partial Charges

method/basis	CH ₄		HCN		
	C	H	H	C	N
IAO/def2-SVP ^a	-0.49	+0.12	+0.21	-0.01	-0.20
IAO/def2-TZVPP ^a	-0.52	+0.13	+0.22	-0.01	-0.21
IAO/def2-QZVPP ^a	-0.52	+0.13	+0.22	-0.01	-0.21
IAO/cc-pVTZ ^a	-0.52	+0.13	+0.22	-0.01	-0.21
IAO/aug-cc-pVTZ ^a	-0.52	+0.13	+0.22	-0.01	-0.21
Bader/TZ2P ^b	+0.05	-0.01	+0.19	+0.82	-1.01
Mulliken/DZ ^b	-0.98	+0.25	+0.34	+0.03	-0.38
Mulliken/DZP ^b	+0.05	-0.01	+0.16	+0.28	-0.44
Mulliken/TZ2P ^b	+0.61	-0.15	-0.02	+0.27	-0.25
IAO/cc-pVTZ ^c	-0.49	+0.12	+0.22	-0.03	-0.19
IAO/cc-pVTZ ^d	-0.49	+0.12	+0.21	-0.03	-0.18

^aHartree–Fock partial charges via eq 3; ^bKohn-Sham/BP86 partial charges⁶ via the Bader and Mulliken methods; ^cHartree–Fock partial charges, using Huzinaga MINI³² for basis B_2 instead of MINAO (see Appendix B); and ^dHartree–Fock partial charges with B_2 functions taken from ANO-RCC.^{33,34}

charges obtained are insensitive to the basis set and follow trends in electronegativities; in addition, some defects seen in other methods (e.g., Bader's description of the CN bond in HCN as ionic) are absent. Partial charges will be further analyzed below.

IAOs provide access to atomic properties, but it is often desirable to get a clearer picture of molecular bonding. We now show that, by combining the IAOs with orbital localization in the spirit of Pipek–Mezey (PM),³⁵ one can explicitly construct bond orbitals (IBOs), without any empirical input, and *entirely within the framework of MO theory*. A Slater determinant $|\Phi\rangle$ is invariant to unitary rotations $|i'\rangle = \sum_i |i\rangle U_{ii'}$ among its occupied MOs $|i\rangle$. We can thus define the IBOs by maximizing

$$L = \sum_A^{\text{atoms}} \sum_{i'}^{\text{occ}} [n_A(i')]^4 \quad (4)$$

with respect to $U_{ii'}$. Here, $n_A(i')$ is the number of electrons from $|i'\rangle$ located on the IAOs ρ of atom A:

$$n_A(i') = 2\sum_{\rho \in A} \langle i' | \rho \rangle \langle \rho | i' \rangle$$

This construction effectively minimizes the number of atoms upon which an orbital is centered. Technical notes (e.g., on the choice of the exponent “4”) and an explicit algorithm to perform the optimization are given in Appendix D.

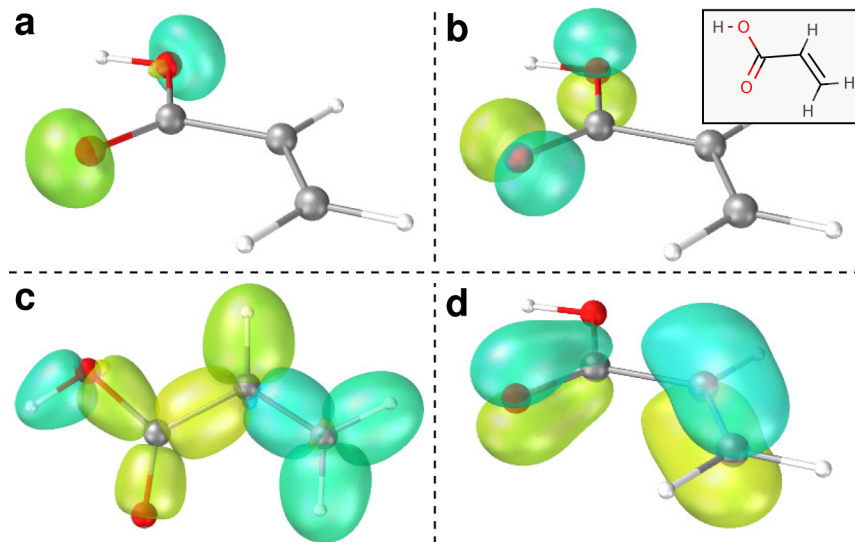


Figure 1. Intrinsic bond orbitals (IBOs) of acrylic acid: (a, b) two sp -hybrid and two p lone pairs (1-center orbitals); (c, d) eight σ -bonds and two π -bonds (2-center orbitals). Core orbitals are not shown. There are a total of 19 IBOs, expanded over 29 IAOs (5 for each C and O atom, and 1 for each H atom; each IAO is in turn expanded over 211 B1 basis functions (def2-TZVPP)).

Figure 1 shows IBOs computed for the acrylic acid molecule. Here, 16 of 19 occupied MOs can be expressed to >99% by charge with IAOs on one or two centers, respectively. The three other MOs are part of a π -system: the oxygen p lone pairs (which have ~7% bonding character), and the C=C π -bond (which has ~3% contributions on the third C atom, and ~1% on the doubly bonded O). In total, we see a direct correspondence of the obtained IBOs with the classical bonding picture: σ -bonds, π -bonds, and lone pairs are exactly where expected, and the π -system is slightly delocalized. We stress again that these 19 IBOs are *exactly equivalent* to the occupied MOs from which they are generated: Their antisymmetrized product is the SCF wave function, and this is a valid representation of its electronic structure. Note that the IBO construction makes no reference to the molecule's Lewis structure whatsoever; the classical bonding picture thus arises as an emergent phenomenon rooted in the molecular electronic structure itself, even if not imposed.

The major improvement of IBOs over PM orbitals is that they are based on IAO charges instead of the erratic Mulliken charges (cf. CH₄ in Table 1). As a result, IBOs are always well-defined, while PM orbitals are unsuitable for interpretation because they are unphysically tied to the basis set¹⁹ (they do not even *have* a basis set limit). IBOs lift this weakness while retaining and even improving on PM's computational attractiveness.

3. CONSISTENCY WITH EMPIRICAL FACTS

Our hypothesis is that IAOs offer a chemically sound definition of atoms in a molecule. However, since these are not physically observable, this claim can only be backed by consistency with empirical laws and facts.³⁶ We thus now investigate whether partial charges derived from IAOs follow expected trends based on electronegativities, C 1s core level shifts, and linear free-energy relationships for resonance substituent effects (Taft's σ_R). We then go on to see how IBOs reflect bonding in some nontrivial molecules (section 3.2), and how coordination complex oxidation states manifest themselves in terms of IAOs (section 3.3).

3.1. Partial Charges: Electronegativities, Core Level Shifts, and Substituent Effects. In Table 1, we saw that,

unlike Mulliken charges, IAO charges are insensitive to the employed basis set, and unlike Bader charges, IAOs do not erroneously describe the CN bond in HCN as being ionic. We now follow ref 6 and investigate IAO charges in relation to differences in electronegativity (χ). We start with the series CH₃X (X = F, Cl, Br, H). Because of the electronegativities (F, 4.193; Cl, 2.869; Br, 2.685; C, 2.544; H, 2.300; taken from the work of Allen³⁷), we expect halogens to have a negative charge, getting smaller in the series, and hydrogen to have a positive charge. As shown in Figure 2a, this is what we find.

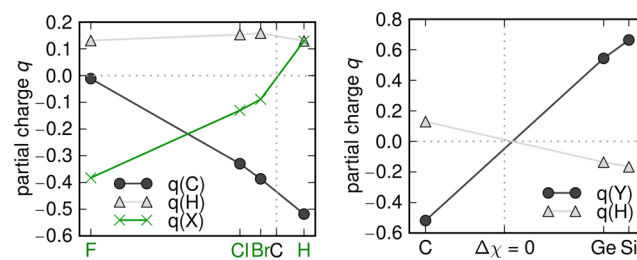


Figure 2. (a) Intrinsic atomic orbital (IAO) partial charges in CH₃X (X = F, Cl, Br, H) plotted against $\chi(C)-\chi(X)$. $\Delta\chi = 0$ is marked by a dotted line. (b) Partial charges in YH₄ (Y = C, Si, Ge); the x-axis is $\chi(H)-\chi(Y)$.

In Figure 2b, we show the series YH₄ (Y = C, Si, Ge). We find charges in close correspondence with χ (C, 2.544; Si, 1.916; Ge, 1.994), and the inversion that $\chi(\text{Si}) < \chi(\text{Ge})$ is properly reflected. If we extrapolate the curves in Figures 2a and 2b to $\Delta\chi = 0$, we find, in both cases, that $q(X) \approx 0$ and $q(Y) \approx 0$, respectively. That is, if there is no difference in electronegativity, IAO partial charges predict no bond polarization. This consistency with empirical electronegativities is further reflected in the almost-linear shapes of the curves. In the series CH_{4-n}F_n ($n = 0, \dots, 4$), we find C partial charges of -0.52, -0.01, 0.44, 0.85, 1.23. The charge increase by ~0.5e⁻ per F atom agrees with the understanding of CF bonds in organic chemistry³⁸ and earlier calculations,³⁹ contrary to the much smaller charges found in Hirshfeld and Voronoi deformation density (VDD) analysis.⁶

A different test of IAO charges can be performed by comparing to experimental data which are known to be highly correlated with charge states of specific atoms A. A prime example for this is the C 1s core-level ionization energy shift caused by the molecular environment. This shift can be estimated⁴⁰ as

$$\Delta\text{IP}_{\text{C}1\text{s}} = k \cdot q_{\text{A}} + \sum_{\text{B} \neq \text{A}} \frac{q_{\text{B}}}{\|\mathbf{R}_{\text{A}} - \mathbf{R}_{\text{B}}\|} + \Delta E_{\text{relax}} \quad (5)$$

where the second term is an estimate for the electrostatic potential of the other atoms B, the last term is a contribution due to core orbital relaxation, and k is a (hybridization-dependent) proportionality constant. This model has been employed to calibrate widely used electronegativity equilibration models,⁴¹ and it has been found to be perfectly correlated with both experimental⁴² and theoretical⁴³ mean dipole derivatives (which for the molecules studied here can be interpreted as charges,⁴³ but not generally⁴⁴). In Figure 3, we show the results obtained with

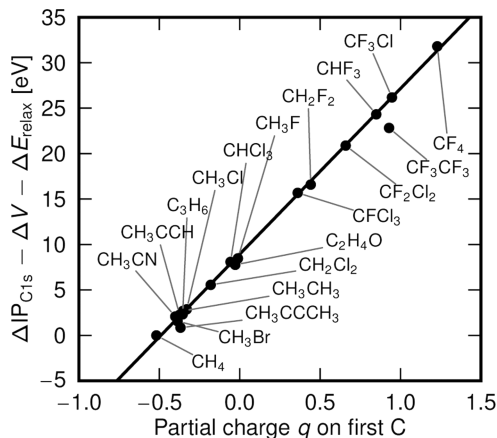


Figure 3. Partial charge on sp^3 carbon versus experimental C 1s ionization energy shift corrected for core relaxation effects and electrostatic potentials of the other cores (eq 5), relative to methane.

IAO partial charges based on Hartree–Fock wave functions for all the sp^3 hybridized molecules studied in ref 42. IAO charges were used both for the abscissa and V , the second term in eq 5. ΔE_{relax} was calculated at Hartree–Fock level by a ΔSCF procedure. Here, we obtain a linear regression coefficient of $r = 0.997$, or $r = 0.9995$ if the two outliers CF_3CF_3 and $\text{CH}_3\text{C}\equiv\text{CH}_3$ are excluded. This is the same level of correlation as obtained with dipole moment derivatives,⁴² and much higher than for CHELPS, Bader, or Mulliken charges.⁴³

One advantage of Hilbert-space based partial charges over real-space partial charges is that they can be split not only into atomic contributions, but also into orbital contributions. Recently, Ozimiński and Dobrowolski⁴⁵ used this freedom to introduce a set of descriptors for the electronic σ - and π -substituent effects, called sEDA and pEDA, and they showed that they are both internally consistent and highly correlated with empirical substituent effect parameters such as Taft's σ_R . Concretely, for a substituted benzene $\text{R}-\text{C}_6\text{H}_5$, the pEDA parameter is defined as the number of p_z electrons on the six carbon atoms of the benzene ring, relative to the unsubstituted benzene:

$$\text{pEDA} = \sum_{i=1}^6 q_{\text{C}_i 2p_z} (\text{C}_6\text{H}_6) - \sum_{i=1}^6 q_{\text{C}_i 2p_z} (\text{R}-\text{C}_6\text{H}_5) \quad (6)$$

where Ozimiński defined this quantity based on NAO population analysis⁴ with a specified type of wave function and basis set. In order to demonstrate the potential of IAO charges in the interpretation of chemical reactivity, in Figure 4 we show that

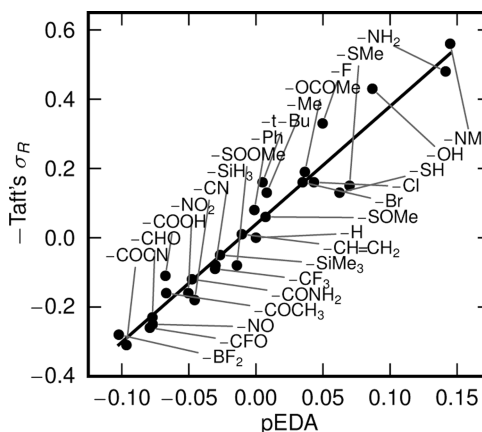


Figure 4. Correlation of pEDA based on IAO/Hartree–Fock charges versus σ_R substituent constants taken from Table IV in ref 47.

the same type of correlation with empirical substituent constants is also obtained when calculating pEDA from IAO charges ($r = 0.966$) instead of NAO charges ($r = 0.943$ ⁴⁵). While Figure 4 still shows considerable scatter, it must be stressed that linear free-energy relationships are not strict laws; rather, they are a form of condensing highly complex interactions into an effective, easy-to-handle descriptor, in order to facilitate predicting reactivity trends. Consequently, neither the accuracy of the relationships themselves is much better than the correlations obtained here (e.g., see Figure 1 in ref 46), nor is the internal consistency of different ways of evaluating its substituent constants (e.g., $r = 0.982$ for σ_R from protonation equilibria versus σ_R from F-NMR shifts of para- and meta-substituted fluorobenzenes; see section 1.D in ref 47). This does not diminish their usefulness.

Calculating such EDA descriptors as obtained here is computationally trivial, which makes them an attractive quantity in the study of unusual substituents not contained in common tables, or for testing if the substituents behave differently for different hosts than benzene. Indeed, an idea similar to Ozimiński's has been considered previously;⁴⁸ but since Hilbert space approaches were considered unreliable,⁴⁸ it was based on carefully crafted real-space integration, and thus much less practical.

3.2. Nontrivial Bonding in Terms of Bond Orbitals. A deeper insight into the nature of a molecule's bonding can be obtained by calculating its bond orbitals. As previously noted, IBOs are an *exact* representation of SCF wave functions, and we have seen in Figure 1 that they normally reflect the classical bonding concepts one to one. However, in many molecules the Lewis structure does not tell the entire story. Therefore, we now probe how IBOs reflect bonding in some well-known, but in different senses nontrivial molecules.

Benzene. A straight application of the IBO construction produces the orbitals shown in Figures 5a–e. As expected, both the CC and the CH σ -bonds of the system are completely localized, and can be expressed to >99% with IAOs on only the two bonded centers. As a prototypical delocalized system,

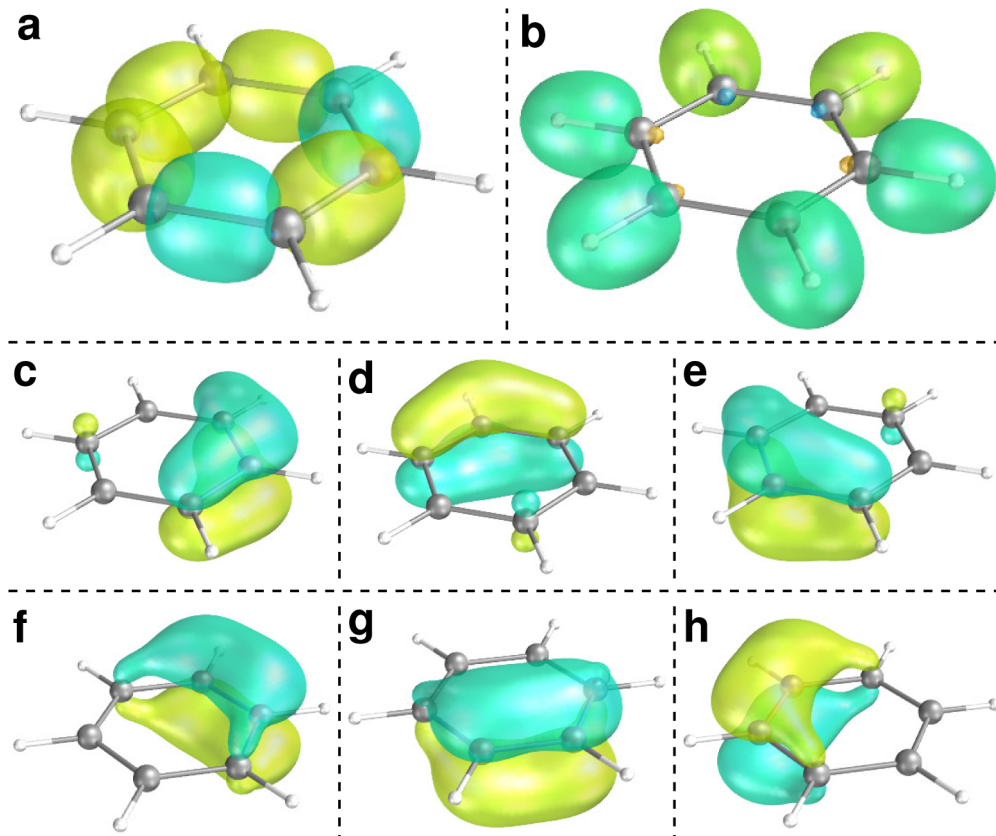


Figure 5. IBOs of benzene: (a) six CC σ -bonds and (b) six CH σ -bonds, both localized; and (c–e) one of the two equivalent IBO sets representing the delocalized π -system of three orbitals. (f–h): See text.

this does, however, not hold for the π system. Two aspects are important:

- (i) The three π orbitals cannot be expressed with IAOs on less than four centers each (in Figures 5c, 5d, and 5e having the weights 1.000, 0.444 (ortho), and 0.111 (para)), respectively.
- (ii) There are two different maximal localizations of the functional given in eq 4: the orbitals shown in Figures 5c–e and the orbitals in Figures 5c–e rotated by 60° in real space.

If, in eq 4, we had chosen to maximize $\sum n_A(i)^2$ instead of $\sum n_A(i)^4$, there would even be a continuum of maximal localizations, also including the orbitals described by Figures 5f–h (which look closer to classical π -bonds), and everything in between. Both types of local π -orbitals have been discussed by England and co-workers.⁴⁹ In this case, the classical resonance structure reflects the nature of the bonding well.

Cyclopropane. According to its Lewis structure, cyclopropane is a simple alkane. However, one could expect that the massive ring strain must have some impact on the bonding. Nevertheless, if we calculate the IBOs of this molecule (see Figures 6a and 6b), we find six CH single bonds and three CC single bonds, all perfectly localized (to >99%) on the two bonded centers, with no delocalization whatsoever. However, a closer look reveals that, although the carbon part of the CH bond orbitals has ~28% s-character and 72% p-character, (close to the ideal sp^3 hybrid values of $\frac{1}{4}s + \frac{3}{4}p$), the CC bonds only have 18% s-character and 82% p-character. So, although they are localized single bonds, they must be considered as an intermediate between a regular sp^3 -hybrid σ -bond and a

π -bond. This explains the well-known similarity in reactivity to alkenes.⁵⁰ The bent bonds have previously been discussed in refs 50–52 and references therein.

Diborane. B_2H_6 has been a serious challenge to the classical bonding picture, with even scientists such as Pauling championing an ethane-like structure until proven wrong irrefutably.⁵³ Its bridged structure was popularized in 1943,⁵⁴ and it spawned investigations culminating in Lipscomb's 1976 Nobel prize for his "studies on the structure of boranes illuminating problems of chemical bonding". One could think that this molecule presents a challenge to a IBO bonding analysis. However, IBOs are just the most local exact description of a first-principles wave function, and their construction does not make *any* reference to *any* perceived nature of the bonding. Consequently, for IBO analysis diborane is not different than other molecules, and it uncovers diborane's two two-electron three-center bonds (Figure 6d) just as its six standard σ -bonds (described by Figure 6c), without any problems.

Sulfur Trioxide. SO_3 is one of the simplest "hypervalent" molecules, apparently violating the octet rule. While a direct d -orbital bonding has been ruled out,^{55–57} hypervalent species remain a debated topic to this day.^{58–60} An IBO analysis of SO_3 finds two oxygen lone pairs, one σ - and one π -bond (see Figure 6e) per oxygen. Formally, this calls for describing the SO bonds as double bonds. However, the π -bonds have only a small bonding component (83% on oxygen, 15% on sulfur), so it is a matter of taste whether they should be called true π -bonds or not. However, in any case, they are highly localized (98% on two centers) and clearly not resonating, so the resonance structure commonly found in textbooks,

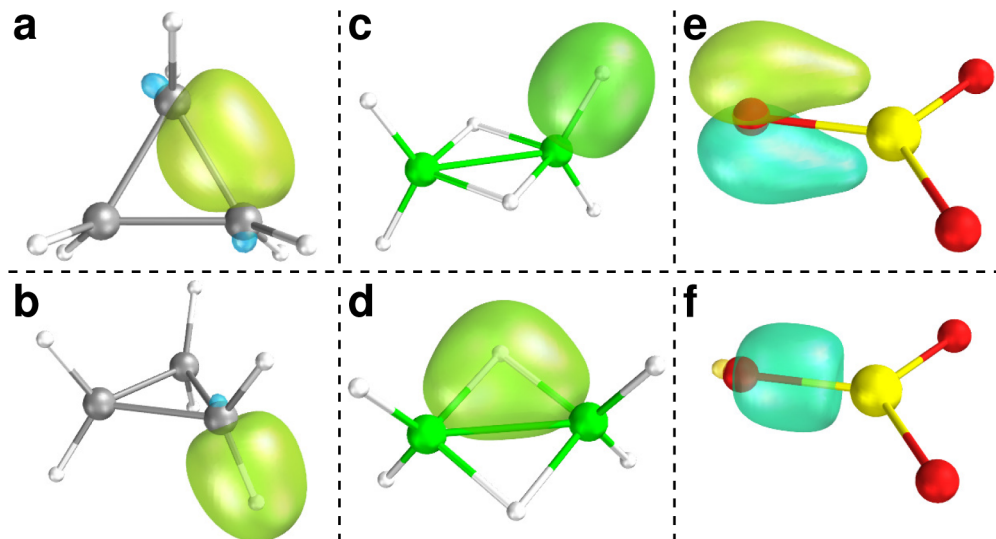
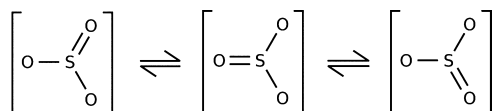


Figure 6. IBO of some molecules with non-Lewis bonding: (a) CC banana bond and (b) CH σ -bond of cyclopropane; (c) BH σ -bond; (d) BHB 2e3c bond of diborane; (e) SO π -bond; and (f) SO σ -bond of sulfur trioxide.



is, at best, misleading. [Three double bonds are allowed here because they are polar, and thus contribute less than one electron per bond to sulfur's valence orbitals. Consequently, two electrons per valence orbital are never exceeded (the quantum mechanical core of the octet rule) and neither delocalization nor d -orbital participation need to be invoked.] While also the present picture results in a bond order of ~ 1.3 , here the bonds are static and near uncorrelated with each other, unlike in a truly delocalized system such as benzene. The simple bonding picture consisting of polar two-center bonds has also been obtained by Cunningham and co-workers in a valence bond analysis.⁵⁷

Bifluoride Anion. We see a similar discrepancy to textbook knowledge in the description of the bifluoride anion, FHF^- . This molecule, which is still actively researched,^{61–64} is alternatively cited as the strongest known hydrogen bond,⁶⁵ or as an example for a 4-electron 3-center (4e3c) bond (since an influential paper by Pimentel⁶⁶). However, IBO analysis reveals that it can be perfectly described by six F lone pairs and two HF single bonds, all completely localized. Since the bonds are very polar, there is again no violation of the octet rule. In fact, the H orbital has a population of only 0.6 electrons total (out of the maximum of two electrons that it theoretically could harbor), and the nature of bonding in this molecule is not very different than in HF. The fact that such “4e3c” bonds are often just two polar 2e2c bonds was previously noted by Ponec and co-workers,⁶⁷ but this view is not yet generally accepted.^{58,69}

3.3. Oxidation States of Transition-Metal Complexes.

The occupancies of individual orbitals, as provided by IAOs, can also be employed to define the oxidation states of coordinated transition metals (TMs). This may seem surprising because oxidation states are known to be a vague concept,⁷⁰ and it is well-established that no simple relationship to partial charges exists.^{71–73} However, Sit and co-workers recently introduced an interesting perturbative argument which may elucidate the situation, at least for weakly bonded TMs.⁷⁴

For a free, isolated TM ion, the oxidation state is unambiguously defined (as its ionic charge), and the ion's d-spin orbitals

are either fully occupied ($n = 1$) or fully unoccupied ($n = 0$). Sit and co-workers⁷⁴ then argued that (i) only the fully occupied d-spin orbitals are relevant for determining the oxidation state of the TMs, and (ii) this remains to be the case in a coordinated environment. While some overlap of these d-orbitals with ligand orbitals may occur, it is normally weak, and thus the bonding and antibonding orbitals formed between the TM and the ligand are occupied equally. Consequently, a d-orbital with occupation $n = 1.0$ in the free ion remains at $n \approx 1.0$ in the complex, while all other d-orbital occupations result from ligand donation⁷³ to (and bonding with) previously empty d-orbitals. We can thus find the free ion corresponding to a coordinated TM, and therefore its oxidation state, by simply counting the number of d-spin orbitals with $n \approx 1.0$. This analysis contains two assumptions: (i) the ligands should not be able to withdraw d electrons from the TM instead of bonding to them and (ii) the occupation numbers of the d electrons can be identified.

To address (ii), Sit and co-workers⁷⁴ employed a projection onto unpolarized free-ion d AOs, which were also not orthogonalized to other orbitals. IAOs might provide a better basis for obtaining such occupations, because they take environment polarization into account and they partition all electrons of the molecule into atomic contributions, without double-counting or missing electrons. In the IAO basis, one can thus simply diagonalize the TM's 5×5 d-orbital block of the spin-orbital density matrix in order to obtain the sought after occupation numbers (for alpha and beta spin separately), or, alternatively, see how many IBOs fully localize to the TM center. We here applied the diagonalization method to the TM clusters studied in ref 75. These are the octahedral ML_6 clusters, with M = V(II), Mn(II), Mn(III), Fe(II), Fe(III), Ni(II), and Zn(II), combined with ligands L = Cl^- , H_2O , CN^- , and CO. For Cl^- (a weak-field ligand), only high-spin complexes are considered; for CN^- and CO (both strong-field ligands), only low-spin complexes are considered; and for H_2O , both high-spin and low-spin calculations are performed. The results are reported in Table 2. In all complexes, we see a clear distinction between the fully and nonfully occupied d-orbitals (in most cases, occupations *very close* to 1.0 are obtained), and the number of such $n \approx 1$ orbitals is perfectly consistent with the formal oxidation state, as predicted by Sit and co-workers.⁷⁴ The largest

Table 2. IAO d-Orbital Occupations of Octahedral ML_6 Coordination Complexes^a

complex	S_z	d-orbital occupation					complex	S_z	d-orbital occupation				
Fe(II); expected 6 singly occupied d-orbitals													
$[\text{FeCl}_6]^{4-}$ (spin 4)	A	1.00	1.00	1.00	1.00	1.00	$[\text{V}(\text{CN})_6]^{4-}$ (spin 3)	A	0.94	0.94	0.94	0.19	0.19
	B	1.00	0.06	0.06	0.01	0.01		B	0.19	0.19	0.01	0.01	0.01
$[\text{Fe}(\text{H}_2\text{O})_6]^{2+}$ (spin 0)	A	1.00	1.00	1.00	0.06	0.06	$[\text{V}(\text{CO})_6]^{2+}$ (spin 3)	A	0.90	0.90	0.90	0.25	0.25
	B	1.00	1.00	1.00	0.06	0.06		B	0.25	0.25	0.01	0.01	0.01
$[\text{Fe}(\text{H}_2\text{O})_6]^{2+}$ (spin 4)	A	1.00	1.00	1.00	1.00	1.00	Mn(II); expected 5 singly occupied d-orbitals						
	B	1.00	0.05	0.05	0.01	0.01	$[\text{MnCl}_6]^{4-}$ (spin 5)	A	1.00	1.00	1.00	1.00	1.00
$[\text{Fe}(\text{CN})_6]^{4-}$ (spin 0)	A	0.97	0.97	0.97	0.21	0.21		B	0.05	0.05	0.01	0.01	0.01
	B	0.97	0.97	0.97	0.21	0.21	$[\text{Mn}(\text{H}_2\text{O})_6]^{2+}$ (spin 1)	A	1.00	1.00	1.00	0.05	0.05
$[\text{Fe}(\text{CO})_6]^{2+}$ (spin 0)	A	0.93	0.93	0.93	0.31	0.31		B	1.00	1.00	0.05	0.05	0.01
	B	0.93	0.93	0.93	0.31	0.31	$[\text{Mn}(\text{H}_2\text{O})_6]^{2+}$ (spin 5)	A	1.00	1.00	1.00	1.00	1.00
Fe(III); expected 5 singly occupied d-orbitals													
$[\text{FeCl}_6]^{3-}$ (spin 5)	A	1.00	1.00	1.00	1.00	1.00	$[\text{Mn}(\text{CN})_6]^{4-}$ (spin 1)	A	0.98	0.96	0.96	0.20	0.19
	B	0.15	0.15	0.03	0.03	0.03		B	0.96	0.96	0.20	0.19	0.01
$[\text{Fe}(\text{H}_2\text{O})_6]^{3+}$ (spin 1)	A	1.00	1.00	1.00	0.13	0.11	$[\text{Mn}(\text{CO})_6]^{2+}$ (spin 1)	A	0.94	0.90	0.90	0.32	0.30
	B	1.00	1.00	1.00	0.13	0.11		B	0.90	0.90	0.32	0.30	0.01
$[\text{Fe}(\text{H}_2\text{O})_6]^{3+}$ (spin 5)	A	1.00	1.00	1.00	1.00	1.00	Mn(III); expected 4 singly occupied d-orbitals						
	B	0.09	0.09	0.03	0.02	0.01	$[\text{MnCl}_6]^{3-}$ (spin 4)	A	1.00	1.00	1.00	1.00	0.20
$[\text{Fe}(\text{CN})_6]^{3-}$ (spin 1)	A	0.99	0.99	0.99	0.33	0.28		B	0.20	0.11	0.02	0.02	0.02
	B	0.99	0.99	0.99	0.33	0.28	$[\text{Mn}(\text{H}_2\text{O})_6]^{3+}$ (spin 2)	A	1.00	1.00	1.00	0.11	0.09
$[\text{Fe}(\text{CO})_6]^{3+}$ (spin 1)	A	0.98	0.96	0.96	0.41	0.37		B	1.00	0.11	0.09	0.02	0.01
	B	0.96	0.96	0.96	0.41	0.37	$[\text{Mn}(\text{H}_2\text{O})_6]^{3+}$ (spin 4)	A	1.00	1.00	1.00	1.00	0.11
Ni(II); expected 8 singly occupied d-orbitals													
$[\text{NiCl}_6]^{4-}$ (spin 2)	A	1.00	1.00	1.00	1.00	1.00	$[\text{Mn}(\text{CN})_6]^{3-}$ (spin 2)	A	0.99	0.99	0.98	0.29	0.26
	B	1.00	1.00	1.00	0.05	0.05		B	0.98	0.29	0.26	0.01	0.01
$[\text{Ni}(\text{H}_2\text{O})_6]^{2+}$ (spin 2)	A	1.00	1.00	1.00	1.00	1.00	$[\text{Mn}(\text{CO})_6]^{3+}$ (spin 2)	A	0.97	0.97	0.95	0.38	0.36
	B	1.00	1.00	1.00	0.05	0.05		B	0.95	0.38	0.36	0.02	0.02
$[\text{Ni}(\text{CN})_6]^{4-}$ (spin 2)	A	1.00	1.00	0.99	0.99	0.99	Zn(II); expected 10 singly occupied d-orbitals						
	B	0.99	0.99	0.99	0.20	0.20	$[\text{ZnCl}_6]^{4-}$ (spin 0)	A	1.00	1.00	1.00	1.00	1.00
$[\text{Ni}(\text{CO})_6]^{2+}$ (spin 2)	A	0.99	0.99	0.97	0.97	0.97		B	1.00	1.00	1.00	1.00	1.00
	B	0.97	0.97	0.97	0.28	0.28	$[\text{Zn}(\text{H}_2\text{O})_6]^{2+}$ (spin 0)	A	1.00	1.00	1.00	1.00	1.00
V(II); expected 3 singly occupied d-orbitals													
$[\text{VCl}_6]^{4-}$ (spin 3)	A	1.00	1.00	1.00	0.12	0.12	$[\text{Zn}(\text{CN})_6]^{4-}$ (spin 0)	A	1.00	1.00	1.00	1.00	0.88
	B	0.12	0.12	0.03	0.03	0.03		B	1.00	1.00	1.00	1.00	0.88
$[\text{V}(\text{H}_2\text{O})_6]^{2+}$ (spin 3)	A	1.00	1.00	1.00	0.07	0.07	$[\text{Zn}(\text{CO})_6]^{2+}$ (spin 0)	A	1.00	1.00	0.99	0.99	0.99
	B	0.07	0.07	0.02	0.01	0.01		B	1.00	1.00	0.99	0.99	0.99

^aShown are the eigenvalues of the 5×5 block of the alpha-spin (A) and beta-spin (B) density matrices. Sub-captions note the number of fully occupied d-orbitals expected for a TM of the given oxidation state.⁷⁴ Orbital occupations that we regard as near 1.0 are highlighted in bold font.

deviations are seen for the CO ligand; this may be related to CO's strong π -acceptor properties, which could cause a violation of condition (i) mentioned above. But, in any case, the assignment of oxidation states appears to be straightforward and unambiguous for the complexes considered here. The combination of the analysis by Sit and co-workers⁷⁴ with the IAO technique proposed here may thus offer a useful method for classifying oxidation states also in less-transparent complexes.

4. CONCLUSIONS AND OUTLOOK

The proposed intrinsic atomic orbitals (IAOs) offer a simple and transparent way to relate chemical intuition to quantum chemistry. In particular, the fact that most simple bonds can be expressed to >99% with IAOs on only two atoms strongly indicates that IAOs can be interpreted as *chemical valence orbitals* in molecules. That properties of individual such orbitals can then be directly calculated, as shown in Figure 4, may turn out to be a decisive factor in future research on chemical reactivity. Similarly, IAOs may greatly simplify the construction of realistic tight-binding model Hamiltonians and their use in elucidating complex correlated electronic structure phenomena.^{76,77}

The proposed intrinsic bond orbitals (IBOs) can help to uncover the nature of bonding in molecules; because of their unbiased nature, this also applies in unusual cases. However, the IBO construction's simplicity, ease of implementation, and high runtime efficiency make it an excellent choice also where localized orbitals are used for purely technical reasons (e.g., in local electron correlation methods).

APPENDIX

A. Availability of the Intrinsic Atomic Orbital (IAO) and Intrinsic Bond Orbital (IBO) Techniques

The techniques have been implemented into the development version of Molpro and will become available with its next public release. In addition, a complete example implementation of the IAO and IBO constructions will be made available at <http://www.theochem.uni-stuttgart.de/~knizia/> (Python source).

B. Notes on the Free-Atom Atomic Orbitals

Effectively, the only empirical input to the entire IAO/IBO construction is the choice of the atomic state from which the free-atom atomic orbitals (AOs) are calculated. For the data presented in the paper (except for the transition metals (TMs) in Table 2),

we used spherically averaged ground-state Hartree–Fock orbitals; these were simply taken from the contracted functions of the cc-pVTZ basis sets^{78–80} (the set is called “MINAO” in Molpro). These AOs are sufficiently accurate for the present purpose, but in principle one could recalculate them with a larger freedom in the radial space of the occupied AOs. For pragmatic reasons, we used minimal basis subsets of cc-pVTZ⁸¹ also for the TMs; however, in this case, cc-pVTZ is derived from averages over important states instead of only ground states.⁸¹ The impact of this choice should be checked at a later point in time.

While one could argue for using AOs from a promoted state⁸² or valence state,⁸³ here we prefer the ground state as reference. This choice is made mainly because it is both observable and unique, and because this way the presented theory obtains the property of generalized observability as defined by Cioslowski and Surjan.⁸⁴ Initial numerical experiments indicated that, in most cases, neither choice (ground state, valence state, or promoted state) makes a large difference to results obtained via IAO analysis, and that the presented method is less sensitive to the choice of the free-atom state than Hirshfeld or VDD methods.⁶ However, some further research on how to best deal with cases in which the atomic character in the molecule differs considerably from the ground state may be warranted.

C. Technical Notes on the IAO Construction

The explicit matrix form of the projector P_{12} for contra-variant indices (such as the basis function index of orbital coefficients) is

$$\mathbf{P}_{12} = \mathbf{S}_1^{-1} \mathbf{S}_{12}$$

where $[\mathbf{S}_1]_{\mu\nu} = \langle \mu|\nu \rangle$ ($\mu, \nu \in B_1$) is the overlap matrix within basis B_1 and $[\mathbf{S}_{12}]_{\mu\sigma} = \langle \mu|\sigma \rangle$ ($\mu \in B_1, \sigma \in B_2$) the overlap matrix between B_1 and B_2 . An explicit proof of this form can be found in eq 3 of ref 85 (note that a projector to a space Y is defined by mapping any point x to its closest point $y \in \text{span}(Y)$, i.e., $Px = \text{argmin}_{y \in Y} \|x - y\|_2$), but it also can be easily seen by considering the index form $C_i^\mu = \sum_{\nu\sigma} S^{\mu\nu} S_{\nu\sigma} C_i^\sigma$, where the inverse overlap matrix $S^{\mu\nu} \equiv [\mathbf{S}_1^{-1}]_{\mu\nu}$ within B_1 is used to convert one index (ν) back from covariant to contra-variant. (See ref 86 for an in-depth discussion of the nonorthogonal tensor formalism in the context of quantum chemistry.) The projector P_{21} is obtained by exchanging all indices 1, 2. Note that if the main basis B_1 is sufficiently large (as is normally the case), the vectors from B_2 can be expressed almost exactly in B_1 ; thus, P_{12} is very close to the identity operator and only included for completeness.

Let \mathbf{C} denote the orbital coefficient matrix of $|i\rangle = \sum_\mu |\mu\rangle C_i^\mu$. Then, the matrix form of eqs 1 and 2 become

$$\tilde{\mathbf{C}} = \text{orth}(\mathbf{S}_1^{-1} \mathbf{S}_{12} \mathbf{S}_2^{-1} \mathbf{S}_{21} \mathbf{C})$$

$$\mathbf{A} = \mathbf{C} \mathbf{C}^T \mathbf{S}_1 \tilde{\mathbf{C}} \tilde{\mathbf{C}}^T \mathbf{S}_1 \mathbf{P}_{12} + (1 - \mathbf{C} \mathbf{C}^T \mathbf{S}_1)(1 - \tilde{\mathbf{C}} \tilde{\mathbf{C}}^T \mathbf{S}_1) \mathbf{P}_{12}$$

The orthonormalization is defined as

$$\text{orth}(\mathbf{C}) = \mathbf{C} [\mathbf{C}^T \mathbf{S}_1 \mathbf{C}]^{-1/2}$$

where $\mathbf{X}^{-1/2}$ denotes the matrix inverse square root (however, the procedure is invariant to the concrete type of orthogonalization used). The resulting $[\mathbf{A}]_\rho^\mu$ is the coefficient matrix of the not-yet-orthogonal IAO $|\rho\rangle = \sum_\mu |\mu\rangle A_\rho^\mu$ ($\mu \in B_1, \rho \in B_2$). Here, ρ should be considered as an index of the free-atom AO to which the perturbed AO $|\rho\rangle$ corresponds. The vectors \mathbf{A} are subsequently multiplied by $[\mathbf{A}^T \mathbf{S}_1 \mathbf{A}]^{-1/2}$ from the right to arrive at a symmetrically orthogonalized set of IAO coefficients.

For applications where runtime performance or formula simplicity is of utmost importance (such as in analytic gradients), the simpler formula $\mathbf{A} \approx (\mathbf{S}_1^{-1} + \mathbf{C} \mathbf{C}^T - \tilde{\mathbf{C}} \tilde{\mathbf{C}}^T) \mathbf{S}_{12}$ may also be useful. This formula also leads to a set of AOs that spans the occupied space and gives very similar results in practice. However, it would be obtained if eq 2 were replaced by

$$\begin{aligned} |\rho\rangle &= (1 + \mathbf{O} - \tilde{\mathbf{O}})|\tilde{\rho}\rangle \\ &= (\mathbf{O}\tilde{\mathbf{O}} + (1 + \mathbf{O})(1 - \tilde{\mathbf{O}}))|\tilde{\rho}\rangle \end{aligned}$$

and, thus, can be seen to polarize the virtual space in the wrong direction.

We note that actual inverse overlap matrices should not be used, because this could lead to numerical problems if large or diffuse basis sets were used.⁸⁷ Rather, $\mathbf{X} = \mathbf{S}^{-1} \mathbf{B}$ is a shorthand notation for “solve $\mathbf{S}\mathbf{X} = \mathbf{B}$ ” using a Choleksy or spectral decomposition of \mathbf{S} . Alternatively, twice multiplying with $\mathbf{S}^{-1/2}$ instead of once with \mathbf{S}^{-1} is also numerically stable.⁸⁷

Let us now discuss why $|\rho\rangle$ of eq 2 spans the occupied space of the MOs. Let $\tilde{\mathbf{O}} = \sum_i |\tilde{i}\rangle \langle \tilde{i}|$ and $\mathbf{O} = \sum_i |i\rangle \langle i|$ as defined previously. Then $1 = \tilde{\mathbf{O}} + (1 - \tilde{\mathbf{O}})$ is a resolution of the identity in the space spanned by $\{P_{12}|\rho\rangle, \rho \in B_2\}$, and both span $\{\tilde{\mathbf{O}}P_{12}|\rho\rangle\}$ and span $\{(1 - \tilde{\mathbf{O}})P_{12}|\rho\rangle\}$ are subspaces of certain integer dimension. If we now form span $\{\mathbf{O}\tilde{\mathbf{O}}P_{12}|\rho\rangle\}$ (first term of eq 2), then this space will span the occupied orbitals, provided that the obtained space has the same dimension as the number of occupied orbitals, n_{occ} . The reason for this is simply that *any* set of orbitals that retains n_{occ} independent directions after projection with $\mathbf{O} = \sum_i |i\rangle \langle i|$ will have this property. In the current case, this is a very weak requirement, effectively saying that the molecular wave function can be described, to some degree, in terms of free-atom AOs. In practice, it will always be given for valence states. Also, in the concrete form of eq 2, the occupied space projection $\mathbf{O}\tilde{\mathbf{O}}$ is not affected by the second term $(1 - \tilde{\mathbf{O}})(1 - \tilde{\mathbf{O}})$, which acts in the orthogonal subspace and, thus, cannot interfere with the first term.

D. Technical Notes on the IBO Construction

IBOs retain the attractive computational properties that made PM orbitals so successful, and even improve on them. Similar to PM orbitals, IBOs can be obtained by successive 2×2 rotations on the occupied molecular orbitals (MOs).³⁵ For IBOs, this can be done directly in the orthogonal IAO basis; therefore, it is less expensive and better behaved than PM localization, which is done in the full, nonorthogonal basis and can be problematic for large or diffuse basis sets.^{79,88} As for PM orbitals,^{89,90} also for IBOs, the analytic gradient with respect to geometric perturbations can be determined, enabling their use in geometry optimizations.

Concretely, we used the following algorithm for IBO localization. First, the SCF occupied MOs $|i\rangle$, expressed in terms of the original basis B_1 , are transformed to the orthonormal IAO basis via $\mathbf{C}_{\text{IAO}} = \text{orth}(\mathbf{A})^T \mathbf{S}_1 \mathbf{C}$ (with \mathbf{C} as defined in Appendix C). Since the IAOs span the occupied space, this transformation is lossless. Then, a series of unitary transformations among the $|i\rangle$ is performed, as described next, modifying the set of orbital coefficients \mathbf{C}_{IAO} . Finally, the new MOs, now localized, but still expressed via \mathbf{C}_{IAO} in terms of IAOs, are transformed back to B_1 , according to $\mathbf{C}_{B_1} = \text{orth}(\mathbf{A}) \mathbf{C}_{\text{IAO}}$. In total, we thus obtain a new set of localized MOs, expressed in terms of B_1 , which is related by an unitary transformation to the input SCF MOs. Consequently, both MO sets represent the same determinants,

and, thus, any observable property determined from either orbital set is identical.

The iterative optimization is performed as follows: Let $|li\rangle = \sum |\rho\rangle C_i^\rho$ denote the occupied MOs expressed in terms of orthonormal IAOs $|\rho\rangle$ (the C_i^ρ denoting the matrix elements of C_{IAO}). We then iterate the following process: For each occupied orbital pair i, j with $j < i$:

- Set $A_{ij} = 0$ and $B_{ij} = 0$. Then, for each atom X, increment A_{ij} and B_{ij} as either

$$A_{ij} = A_{ij} + 4Q_{ij}^2 - (Q_{ii} - Q_{jj})^2$$

$$B_{ij} = B_{ij} + 4Q_{ij}(Q_{ii} - Q_{jj})$$

(for localization power $p = 2$, as in PM³⁵) or as

$$\begin{aligned} A_{ij} &= A_{ij} - Q_{ij}^4 - Q_{ij}^4 + 6(Q_{ij}^2 + Q_{ij}^2)Q_{ij}^2 \\ &\quad + Q_{ij}^3Q_{jj} + Q_{ii}Q_{ij}^3 \end{aligned}$$

$$B_{ij} = B_{ij} + 4Q_{ij}(Q_{ij}^3 - Q_{ij}^3)$$

(for localization power $p = 4$, as in eq 4), where the charge matrix elements of atom X are defined as

$$Q_{ij} = \sum_{\rho \in X} C_i^\rho C_j^\rho$$

- Calculate the rotation angle $\phi_{ij} = 1/4 \arctan 2(B_{ij}, -A_{ij})$ (where $\arctan 2(y, x) = \arctan(y/x)$ is the two-argument arctangent function, taking the quadrant into account). Then rotate the orbitals $|li\rangle, |lj\rangle$ by

$$\begin{aligned} |li'\rangle &= \cos(\phi_{ij})|li\rangle + \sin(\phi_{ij})|lj\rangle \\ |lj'\rangle &= -\sin(\phi_{ij})|li\rangle + \cos(\phi_{ij})|lj\rangle \end{aligned} \quad (\text{D1})$$

The orbitals are updated in-place; i.e., in the i, j iteration, subsequent pairs i, j already see the rotated orbitals before the entire loop is passed.

The formulas for ϕ_{ij} are obtained by considering the functional $L(\phi_{ij}) = \langle i' | n_X | i' \rangle^p + \langle j' | n_X | j' \rangle^p$, where $|i'\rangle$ and $|j'\rangle$ are defined as in eqs D1 and $p = 2$ or $p = 4$, and then maximizing L with respect to ϕ_{ij} . For $p = 2$, the given ϕ_{ij} exactly maximizes the functional; for $p = 4$, some high-order terms in ϕ_{ij} are neglected.

We found this approach to work exceedingly well in practice and it typically converges in 5 to 10 iterations over all pairs i, j . We believe this to be a consequence of the intrinsic molecular electronic structure, which apparently has a very deep attractor at the localized orbital solution, corresponding to the Lewis structure (where present).

A final comment is required regarding the exponent $p = 4$ in eq 4. In eq 4, we prefer $p = 4$ over the exponent $p = 2$ of PM, because the former leads to discrete localizations in aromatic systems, while the second does not. For example, in benzene, the orbital rotation Hessian has a zero eigenmode if $p = 2$ is used, but not for $p = 4$. For other systems, both exponents lead to effectively identical results. An exponent of $p = 4$ has recently also been found to be effective in diminishing orthogonalization tails in more-traditional orbital localization methods.^{91,92}

E. Methods Used in the Test Calculations

Molecules were built and preoptimized with Avogadro.⁹³ Geometry optimizations were performed with Molpro,⁹⁴ and

employed DF-MP2/aug-cc-pVTZ^{95,96} for the molecules in the discussion of electronegativities and DF-RKS/PBE/def2-TZVPP^{97–99} for everything else. The complexes in Table 2 were not optimized, but average metal–ligand distances were taken from ref 100 and combined with $r_{\text{OH}} = 0.96 \text{ \AA}$, $\alpha_{\text{HOH}} = 104.5^\circ$ (for H_2O), $r_{\text{CN}} = 1.15 \text{ \AA}$ (for CN^-) and $r_{\text{CO}} = 1.15 \text{ \AA}$ (for CO). Geometries and reference values are available upon request.

IAO and IBO calculations were performed either with a development version of Molpro or the demonstration script ibo-ref.py, which is available on the author's homepage. Calculations employed def2-TZVPP⁹⁸ orbital basis sets and univ-JKFIT⁹⁹ fitting basis sets, unless otherwise noted. For Table 2, augmented def2-SVP orbital basis sets were used. Orbital visualizations were produced using Mayavi2.¹⁰¹

In the calculations of the pEDA values, the substituted benzenes were aligned such that the center of the benzene ring lies at the center of the coordinate system, and the x , y , and z axes point into the directions of the principal axes of inertia of its six C atoms. This way the p_z orbitals were maximally aligned along the z -axis, so that their occupation numbers could be directly read off in the population analysis (some of the rings have slight distortions from planarity, but this has an insignificant effect on the obtained results).

■ AUTHOR INFORMATION

Corresponding Author

*E-mail: knizia@theochem.uni-stuttgart.de.

Notes

The authors declare no competing financial interest.

■ ACKNOWLEDGMENTS

We acknowledge funding through ERC Advanced Grant No. 320723 (ASES).

■ REFERENCES

- Harding, M. E.; Vázquez, J.; Gauss, J.; Stanton, J. F.; Kállay, M. *J. Chem. Phys.* **2011**, *135*, 044513.
- Frenking, G.; Krapp, A. *J. Comput. Chem.* **2007**, *28*, 15–24.
- Bader, R. F. *Atoms in Molecules*; Wiley Online Library, 1990.
- Reed, A. E.; Weinstock, R. B.; Weinhold, F. *J. Chem. Phys.* **1985**, *83*, 735.
- Foster, J.; Weinhold, F. *J. Am. Chem. Soc.* **1980**, *102*, 7211–7218.
- Fonseca Guerra, C.; Handgraaf, J.-W.; Baerends, E. J.; Bickelhaupt, F. *M. J. Comput. Chem.* **2004**, *25*, 189–210.
- Reed, A. E.; Weinhold, F. *J. Chem. Phys.* **1985**, *83*, 1736–1740.
- Morokuma, K. *J. Chem. Phys.* **1971**, *55*, 1236–1244.
- Kitaura, K.; Morokuma, K. *Int. J. Quantum Chem.* **1976**, *10*, 325–340.
- Ziegler, T.; Rauk, A. *Inorg. Chem.* **1979**, *18*, 1558–1565.
- Ziegler, T.; Rauk, A. *Inorg. Chem.* **1979**, *18*, 1755–1759.
- Lein, M.; Szabó, A.; Kovács, A.; Frenking, G. *Faraday Discuss.* **2003**, *124*, 365–378.
- Su, P.; Li, H. *J. Chem. Phys.* **2009**, *131*, 014102.
- Mitoraj, M. P.; Michalak, A.; Ziegler, T. *J. Chem. Theory Comput.* **2009**, *5*, 962–975.
- Michalak, A.; Mitoraj, M.; Ziegler, T. *J. Phys. Chem. A* **2008**, *112*, 1933–1939.
- Lu, W. C.; Wang, C. Z.; Schmidt, M. W.; Bytautas, L.; Ho, K. M.; Ruedenberg, K. *J. Chem. Phys.* **2004**, *120*, 2629–2637.
- Davidson, E. R. *J. Chem. Phys.* **1967**, *46*, 3320–3324.
- Roby, K. R. *Mol. Phys.* **1974**, *27*, 81–104.
- Dubillard, S.; Rota, J.-B.; Saue, T.; Faegri, K. *J. Chem. Phys.* **2006**, *124*, 154307.

- (20) Szczepanik, D.; Mrozek, J. *Comput. Theor. Chem.* **2012**, *996*, 103–109.
- (21) Mulliken, R. S. *J. Chem. Phys.* **1962**, *36*, 3428–3439.
- (22) Heinzmann, R.; Ahlrichs, R. *Theor. Chem. Acc.* **1976**, *42*, 33–45.
- (23) Mayer, I. *J. Phys. Chem.* **1996**, *100*, 6249–6257.
- (24) Liu, W.; Li, L. *Theor. Chem. Acc.* **1997**, *95*, 81–95.
- (25) Ruedenberg, K.; Schmidt, M. W.; Gilbert, M. M. *Chem. Phys.* **1982**, *71*, 51–64.
- (26) Lee, M. S.; Head-Gordon, M. *J. Chem. Phys.* **1997**, *107*, 9085–9095.
- (27) Lee, M. S.; Head-Gordon, M. *Int. J. Quantum Chem.* **2000**, *76*, 169–184.
- (28) Auer, A. A.; Nooijen, M. *J. Chem. Phys.* **2006**, *125*, 024104.
- (29) Subotnik, J. E.; Dutoi, A. D.; Head-Gordon, M. *J. Chem. Phys.* **2005**, *123*, 114108.
- (30) Ivanic, J.; Atchity, G.; Ruedenberg, K. *Theor. Chem. Acc.* **2008**, *120*, 281–294.
- (31) Laikov, D. N. *Int. J. Quantum Chem.* **2011**, *111*, 2851–2867.
- (32) Huzinaga, S.; Andzelm, J.; Klobukowski, M.; Radzio-Andzelm, E.; Sakai, Y.; Tatewaki, H. *Gaussian Basis Sets for Molecular Calculations*; Elsevier: Amsterdam, 1984.
- (33) Widmark, P.-O.; Malmqvist, P.-Å.; Roos, B. O. *Theor. Chem. Acc.* **1990**, *77*, 291–306.
- (34) Roos, B. O.; Lindh, R.; Malmqvist, P.-Å.; Veryazov, V.; Widmark, P.-O. *J. Phys. Chem. A* **2004**, *108*, 2851–2858.
- (35) Pipek, J.; Mezey, P. G. *J. Chem. Phys.* **1989**, *90*, 4916.
- (36) Meister, J.; Schwarz, W. *J. Phys. Chem.* **1994**, *98*, 8245–8252.
- (37) Allen, L. C. *J. Am. Chem. Soc.* **1989**, *111*, 9003–9014.
- (38) O'Hagan, D. *Chem. Soc. Rev.* **2007**, *37*, 308–319.
- (39) Wiberg, K. B.; Rablen, P. R. *J. Am. Chem. Soc.* **1993**, *115*, 614–625.
- (40) Siegbahn, K.; Nordling, C.; Johansson, G.; Hedman, J.; Heden, P.; Hamrin, K.; Gelius, U.; Bergmark, T.; Werme, L.; Manne, R.; Baer, Y. *ESCA Applied to Free Molecules*; North-Holland: Amsterdam, 1970.
- (41) Gasteiger, J.; Marsili, M. *Tetrahedron* **1980**, *36*, 3219–3228.
- (42) Guadagnini, P. H.; Oliveira, A. E.; Bruns, R. E.; de Barros Neto, B. *J. Am. Chem. Soc.* **1997**, *119*, 4224–4231.
- (43) de Oliveira, A. E.; Guadagnini, P. H.; Haiduke, R. L.; Bruns, R. E. *J. Phys. Chem. A* **1999**, *103*, 4918–4924.
- (44) Milani, A.; Tommasini, M.; Castiglioni, C. *Theor. Chem. Acc.* **2012**, *131*, 1–17.
- (45) Ozimiński, W. P.; Dobrowolski, J. C. *J. Phys. Org. Chem.* **2009**, *22*, 769–778.
- (46) Hammett, L. P. *J. Am. Chem. Soc.* **1937**, *59*, 96–103.
- (47) Hansch, C.; Leo, A.; Taft, R. *Chem. Rev.* **1991**, *91*, 165–195.
- (48) Wiberg, K. B. *J. Am. Chem. Soc.* **1980**, *102*, 1229–1237.
- (49) England, W.; Salmon, L. S.; Ruedenberg, K. *Molecular Orbitals*; Springer: Berlin, New York, 1971; pp 31–123.
- (50) de Meijere, A. *Angew. Chem., Int. Ed.* **1979**, *18*, 809–826.
- (51) Boatz, J. A.; Gordon, M. S.; Hilderbrandt, R. L. *J. Am. Chem. Soc.* **1988**, *110*, 352–358.
- (52) Wiberg, K. B. *Acc. Chem. Res.* **1996**, *29*, 229–234.
- (53) Laszlo, P. *Angew. Chem., Int. Ed.* **2000**, *39*, 2071–2072.
- (54) Longuet-Higgins, H.; Bell, R. *J. Chem. Soc.* **1943**, 250–255.
- (55) Kutzelnigg, W. *Angew. Chem., Int. Ed.* **1984**, *23*, 272–295.
- (56) Magnusson, E. *J. Am. Chem. Soc.* **1990**, *112*, 7940–7951.
- (57) Cunningham, T. P.; Cooper, D. L.; Gerratt, J.; Karadakov, P. B.; Raimondi, M. *J. Chem. Soc., Faraday Trans.* **1997**, *93*, 2247–2254.
- (58) Schmøkel, M. S.; Cenedese, S.; Overgaard, J.; Jørgensen, M. R.; Chen, Y.-S.; Gatti, C.; Stalke, D.; Iversen, B. B. *Inorg. Chem.* **2012**, *51*, 8607–8616.
- (59) Grabowsky, S.; Luger, P.; Buschmann, J.; Schneider, T.; Schirmeister, T.; Sobolev, A. N.; Jayatilaka, D. *Angew. Chem., Int. Ed.* **2012**, *51*, 6776–6779.
- (60) Glezakou, V.-A.; Elbert, S. T.; Xantheas, S. S.; Ruedenberg, K. *J. Phys. Chem. A* **2010**, *114*, 8923–8931.
- (61) Sebald, P.; Bargholz, A.; Oswald, R.; Stein, C.; Botschwina, P. *J. Phys. Chem. A* **2013**, *117* (39), 9695–9703.
- (62) Perez-Hernandez, G.; Gonzalez-Vazquez, J.; Gonzalez, L. *J. Phys. Chem. A* **2012**, *116*, 11361–11369.
- (63) Sebald, P.; Oswald, R.; Botschwina, P.; Kawaguchi, K. *Phys. Chem. Chem. Phys.* **2013**, *15*, 6737–6748.
- (64) Stein, C.; Oswald, R.; Sebald, P.; Botschwina, P.; Stoll, H.; Peterson, K. A. *Mol. Phys.* **2013**, *111*, 2647–2652.
- (65) Gilli, G.; Gilli, P. *J. Mol. Struct.* **2000**, *552*, 1–15.
- (66) Pimentel, G. C. *J. Chem. Phys.* **1951**, *19*, 446–448.
- (67) Ponec, R.; Yuzhakov, G.; Cooper, D. L. *Theor. Chem. Acc.* **2004**, *112*, 419–430.
- (68) Bridgeman, A. J.; Empson, C. *J. New J. Chem.* **2008**, *32*, 1359–1367.
- (69) Braida, B.; Hiberty, P. C. *Nat. Chem.* **2013**, *5*, 417–422.
- (70) Jansen, M.; Wedig, U. *Angew. Chem., Int. Ed.* **2008**, *47*, 10026–10029.
- (71) Aullón, G.; Alvarez, S. *Theor. Chem. Acc.* **2009**, *123*, 67–73.
- (72) Resta, R. *Nature* **2008**, *453*, 735–735.
- (73) Raebiger, H.; Lany, S.; Zunger, A. *Nature* **2008**, *453*, 763–766.
- (74) Sit, P. H.-L.; Car, R.; Cohen, M. H.; Selloni, A. *Inorg. Chem.* **2011**, *50*, 10259–10267.
- (75) Thom, A. J.; Sundstrom, E. J.; Head-Gordon, M. *Phys. Chem. Chem. Phys.* **2009**, *11*, 11297–11304.
- (76) Knizia, G.; Chan, G. K.-L. *Phys. Rev. Lett.* **2012**, *109*, 186404.
- (77) Knizia, G.; Chan, G. K.-L. *J. Chem. Theory Comput.* **2013**, *9*, 1428–1432.
- (78) Dunning, T. H., Jr. *J. Chem. Phys.* **1989**, *90*, 1007–1023.
- (79) Dunning, T. H., Jr.; Peterson, K. A.; Wilson, A. K. *J. Chem. Phys.* **2001**, *114*, 9244–9253.
- (80) Prascher, B. P.; Woon, D. E.; Peterson, K. A.; Dunning, T. H., Jr.; Wilson, A. K. *Theor. Chem. Acc.* **2011**, *128*, 69–82.
- (81) Balabanov, N. B.; Peterson, K. A. *J. Chem. Phys.* **2005**, *123*, 064107.
- (82) Mulliken, R. S. *Chem. Rev.* **1931**, *9*, 347–388.
- (83) Ruedenberg, K. *Rev. Mod. Phys.* **1962**, *34*, 326–376.
- (84) Cioslowski, J.; Surján, P. R. *J. Mol. Struct.: THEOCHEM* **1992**, *255*, 9–33.
- (85) Boughton, J. W.; Pulay, P. *J. Comput. Chem.* **1993**, *14*, 736–740.
- (86) Head-Gordon, M.; Maslen, P. E.; White, C. A. *J. Chem. Phys.* **1998**, *108*, 616.
- (87) Knizia, G.; Li, W.; Simon, S.; Werner, H.-J. *J. Chem. Theory Comput.* **2011**, *7*, 2387–2398.
- (88) Mata, R. A.; Werner, H.-J. *Mol. Phys.* **2007**, *105*, 2753–2761.
- (89) Azhary, A. E.; Rauhut, G.; Pulay, P.; Werner, H.-J. *J. Chem. Phys.* **1998**, *108*, 5185–5193.
- (90) Schütz, M.; Werner, H.-J.; Lindh, R.; Manby, F. R. *J. Chem. Phys.* **2004**, *121*, 737–750.
- (91) Jansík, B.; Høst, S.; Kristensen, K.; Jørgensen, P. *J. Chem. Phys.* **2011**, *134*, 194104.
- (92) Høyvik, I.-M.; Jansík, B.; Jørgensen, P. *J. Chem. Theory Comput.* **2012**, *8*, 3137–3146.
- (93) Hanwell, M. D.; Curtis, D. E.; Lonie, D. C.; Vandermeersch, T.; Zurek, E.; Hutchison, G. R. *J. Cheminform.* **2012**, *4*, 1–17.
- (94) Werner, H.-J.; Knowles, P. J.; Knizia, G.; Manby, F. R.; Schütz, M. *WIRE: Comput. Mol. Sci.* **2012**, *2*, 242–253.
- (95) Kendall, R. A.; Dunning, T. H., Jr.; Harrison, R. J. *J. Chem. Phys.* **1992**, *96*, 6796–6806.
- (96) Weigend, F.; Köhn, A.; Hättig, C. *J. Chem. Phys.* **2002**, *116*, 3175.
- (97) Perdew, J. P.; Burke, K.; Ernzerhof, M. *Phys. Rev. Lett.* **1996**, *77*, 3865–3868.
- (98) Weigend, F.; Ahlrichs, R. *Phys. Chem. Chem. Phys.* **2005**, *7*, 3297–3305.
- (99) Weigend, F. *J. Comput. Chem.* **2007**, *29*, 167–175.
- (100) Orpen, A. G.; Brammer, L.; Allen, F. H.; Kennard, O.; Watson, D. G.; Taylor, R. *J. Chem. Soc., Dalton Trans.* **1989**, S1–S83.
- (101) Ramachandran, P.; Varoquaux, G. *Comput. Sci. Eng.* **2011**, *13*, 40–51.

■ NOTE ADDED AFTER ASAP PUBLICATION

This paper posted ASAP on October 17, 2013. Additional corrections were made in Tables 1, 2, Section 3 and the Appendix. The revised version was reposted on October 23, 2013.